



# Strong influenza-induced T<sub>FH</sub> generation requires CD4 effectors to recognize antigen locally and receive signals from continuing infection

Priyadharshini Devarajan<sup>a</sup>, Allen M. Vong<sup>a</sup>, Catherine H. Castonguay<sup>a</sup>, Olivia Kugler-Umana<sup>a</sup>, Bianca L. Bautista<sup>a</sup>, Michael C. Jones<sup>a</sup>, Karen A. Kelly<sup>b</sup>, Jingya Xia<sup>a</sup>, and Susan L. Swain<sup>a,1</sup>

<sup>a</sup>Department of Pathology, University of Massachusetts Medical School, Worcester, MA 01605; and <sup>b</sup>Department of Animal Medicine, University of Massachusetts Medical School, Worcester, MA 01605

Edited by Rafi Ahmed, Emory Vaccine Center, Emory University, Atlanta, GA; received June 15, 2021; accepted December 6, 2021

**While influenza infection induces robust, long-lasting, antibody responses and protection, including the T follicular helper cells (T<sub>FH</sub>) required to drive B cell germinal center (GC) responses, most influenza vaccines do not. We investigated the mechanisms that drive strong T<sub>FH</sub> responses during infection. Infection induces viral replication and antigen (Ag) presentation lasting through the CD4 effector phase, but Ag and pathogen recognition receptor signals are short-lived after vaccination. We analyzed the need for both infection and Ag presentation at the effector phase, using an in vivo sequential transfer model to time their availability. Differentiation of CD4 effectors into T<sub>FH</sub> and GC-T<sub>FH</sub> required that they recognize Ag locally in the site of T<sub>FH</sub> development, at the effector phase, but did not depend on specific Ag-presenting cells (APCs). In addition, concurrent signals from infection were necessary even when sufficient Ag was presented. Providing these signals with a second dose of live attenuated influenza vaccine at the effector phase drove T<sub>FH</sub> and GC-T<sub>FH</sub> development equivalent to live infection. The results suggest that vaccine approaches can induce strong T<sub>FH</sub> development that supports GC responses akin to infection, if they supply these effector phase signals at the right time and site. We suggest that these requirements create a checkpoint that ensures T<sub>FH</sub> only develop fully when infection is still ongoing, thereby avoiding unnecessary, potentially autoimmune, responses.**

T follicular helper cells | T<sub>FH</sub> | influenza | CD4 | vaccination

**T** follicular helper cells (T<sub>FH</sub>) appear late in the CD4 effector response, and they drive the initiation of germinal centers (GCs) and resulting antibody (Ab) production (1). T<sub>FH</sub> are thus essential for strong immune responses generated by influenza infection and vaccines (2–4). Broad, highly protective Ab responses that last many years are generated by natural influenza infection but not by most influenza vaccines (5). Therefore, it is critical that we identify the signals that CD4 T effector cells receive during natural influenza infection that result in their robust differentiation into T<sub>FH</sub> and GC-T<sub>FH</sub>. Such insights could guide the design of superior influenza vaccine strategies and likely vaccines for other RNA viruses, such as HIV and severe acute respiratory syndrome coronavirus 2 (SARS-CoV-2).

After a sublethal dose of influenza infection in mice, viral titers remain at high levels in the lung, from 2 to 8 d postinfection (dpi), and the virus is cleared between 10 and 14 dpi (6). Antigen (Ag) is presented to CD4 T cells for over a week postinfection (7). However, Ag presentation after immunization with an inactivated vaccine is relatively short-lived with most presentation in the initial 3 d after immunization (8). The lack of a sustained Ag recognition and perhaps inflammation generated by ongoing infection may explain why T<sub>FH</sub> development and immunity after infection are far superior to those induced by vaccines (9).

Naive CD4 T cells primed by Ag-presenting cells (APCs) expand and differentiate to become various CD4 effector subsets, including T<sub>FH</sub>. During the effector phase, they clear virus

via multiple synergizing mechanisms before contracting and becoming memory (10, 11). The initial priming requirements for T<sub>FH</sub> generation are well defined (12), but later requirements during the effector phase are not. Once they are generated and enter GCs, T<sub>FH</sub> repeatedly interact with B cells which drives both the GC B cell (GCB) response and further T<sub>FH</sub> differentiation, survival, and expansion (12). Several studies indicate that T<sub>FH</sub> development is enhanced by repeated immunization (13–15), but it is unclear if Ag recognition is required late during the effector phase or where it occurs. A new study suggests that T cell receptor (TCR) affinity for cognate Ag, during the GC response, determines T<sub>FH</sub> affinity, expansion, and contraction (16). Many studies have used in vivo immunization models, but few have analyzed more detailed mechanisms driving T<sub>FH</sub> development during the effector phase following infection.

Moreover, the role of infection, other than supplying Ag presentation for T<sub>FH</sub> development, is unclear. One study showed that effective T<sub>FH</sub> generation during lymphocytic choriomeningitis virus (LCMV) infection required ongoing infection (14), but whether infection supplied Ag or drove inflammation or both was not determined. This is important since vaccines, in a quest for low reactogenicity, often have only mild adjuvant activity. It is not clear what aspects of viral infection, during the

## Significance

**Influenza infection elicits strong, long-lived protective antibodies, but most current influenza vaccines give weaker, short-lived protection. We noted that live virus is still replicating, making antigen and causing inflammation at 7 d postinfection (dpi), while an inactivated vaccine provides antigen for at most 4 dpi. We show that the generation of key T follicular helper cells (T<sub>FH</sub>) requires they recognize antigen locally at 6 dpi in the presence of ongoing viral infection. This creates a checkpoint that restricts T<sub>FH</sub> responses to dangerous infections that persist through the checkpoint. Using a live attenuated vaccine, akin to Flumist, we found that adding a second dose at 6 d generated a strong T<sub>FH</sub> response, suggesting an approach to improve vaccine strategies.**

Author contributions: P.D., A.M.V., and S.L.S. designed research; P.D., A.M.V., C.H.C., O.K.-U., B.L.B., M.C.J., K.A.K., and J.X. performed research; P.D., A.M.V., and O.K.-U. analyzed data; and P.D. and S.L.S. wrote the paper.

The authors declare no competing interest.

This article is a PNAS Direct Submission.

This article is distributed under [Creative Commons Attribution-NonCommercial-NoDerivatives License 4.0 \(CC BY-NC-ND\)](https://creativecommons.org/licenses/by-nc-nd/4.0/).

<sup>1</sup>To whom correspondence may be addressed. Email: [susan.swain@umassmed.edu](mailto:susan.swain@umassmed.edu).

This article contains supporting information online at <http://www.pnas.org/lookup/suppl/doi:10.1073/pnas.2111064119/-DCSupplemental>.

Published February 17, 2022.

effector phase of the immune response, act to drive the strong  $T_{FH}$  development associated with infection. Here, we use an influenza infection model, where strong  $T_{FH}$  responses develop, to identify factors driving  $T_{FH}$  generation at the peak of the CD4 effector phase.

We showed that CD4 effectors generated during influenza A virus (IAV) infection need to recognize Ag during the effector phase at 6 to 8 dpi to escape default apoptosis and effectively form long-lived memory (7, 17). Here, we ask if late steps in the generation of  $T_{FH}$  during infection also require cognate Ag recognition and/or other signals from infection, at this same “effector checkpoint.” We reason that if an infection is quickly cleared, or initial Ag is nonreplicating, both inflammation generated by pathogen recognition and Ag presentation will wane. If those signals are required for  $T_{FH}$  development, it would create a checkpoint that would curtail  $T_{FH}$  responses when infection is cleared and no longer a threat and act as a mechanism to prevent immunopathology and potential autoimmunity.

In this study, we isolate in vivo influenza infection-generated CD4 effectors and transfer them into second hosts where we modulate the availability of cognate Ag and signals from infection. This allows us to pinpoint which signals are required specifically at the CD4 effector phase, during in vivo infection, to induce optimal  $T_{FH}$  generation. We find that CD4 effectors must recognize cognate Ag during the effector phase in spleen and draining lymph node (DLN) sites of  $T_{FH}$  residency, to become full-fledged  $T_{FH}$  including GC- $T_{FH}$ , and that they induce enhanced GCB formation. Multiple types of activated APCs can drive this transition, and it occurs even in the absence of B cells and GC. Moreover, there is an independent requirement for concurrent signals from infection to achieve optimal  $T_{FH}$  generation. Thus, at the effector phase well after initial Ag priming, multiple signals derived from infection act in concert to drive the optimum generation of  $T_{FH}$ . These requirements create a defined checkpoint that regulates  $T_{FH}$  development. Our results from a polyclonal mouse model using live attenuated influenza vaccination to supply these signals suggest that these findings are relevant for designing vaccines that induce stronger  $T_{FH}$  against influenza and likely other life-threatening respiratory viral infections, including the pandemic SARS-CoV-2.

## Results

### Compared to the Inactivated Vaccine, Influenza Infection Provides Extended Ag Presentation through the Initiation of the GC Response.

To understand the factors driving strong protection after infection compared to weaker protection from vaccines, we compared Ag presentation to CD4 T cells in each case. We transferred TCR Tg CD4 T cells that recognize influenza nucleoprotein NP<sub>311–325</sub>, crossed to the Nur77<sup>GFP</sup> reporter, into either influenza-infected mice or mice immunized with whole inactivated influenza (IIV). We analyzed green fluorescent protein (GFP) expression as an indicator of Ag presentation. As expected (7, 8), Ag presentation to CD4 T cells peaked at 5 to 7 dpi and declined slowly thereafter. In contrast, after IIV vaccination, Ag presentation peaked at 3 to 5 d followed by a sharper decline (*SI Appendix, Fig. S1A*).

We analyzed the kinetics of the  $T_{FH}$  and the GC response after influenza infection by transferring naive OT-II CD4 T cells to mice primed with PR8-OVA<sub>II</sub>. At 5 to 6 dpi, few  $T_{FH}$  were detected, they peaked at 7 to 8 dpi, and GCB formed after 6 to 7 dpi (*SI Appendix, Fig. S1 B and C*). Polyclonal CD4 and OT-II responses followed similar kinetics (*SI Appendix, Fig. S1B*). Thus, the peak of Ag presentation after infection (*SI Appendix, Fig. S1A*) correlated with the beginning of the GC response (*SI Appendix, Fig. S1 B and C*) and with the previously defined checkpoint for CD4 effector transition to memory

(7, 17). We hypothesized that the infection and Ag presentation after 6 dpi, which is only weakly provided by IIV, is instrumental in driving superior  $T_{FH}$ -driven immunity. We refer to this timeframe during the CD4 effector phase as the effector checkpoint or the “effector phase” throughout this study.

### An In Vivo Model to Study the Role of Ag Presentation After 6 dpi during the Effector Phase.

We used a sequential transfer approach (7) to manipulate signals available to CD4 effectors (Fig. 1A). We generated 6-dpi CD4 effectors in vivo by transferring naive HNT (specific for IAV hemagglutinin) or OT-II (specific for an OVA epitope) Thy1.1 CD4 T cells (6–8, 17) into primary hosts infected with PR8 or with PR8-OVA<sub>II</sub> (A/PR8/34 engineered to express the OVA<sub>II</sub> determinant in the PR8 hemagglutinin) influenza virus, respectively. After 6 d, we isolated the in vivo-generated donor CD4 effectors and transferred them into second hosts. The second hosts were either uninfected or infected 6 d previously (infection-matched), modeling intact physiology as closely as possible (Fig. 1A). With this model, we can directly control the availability of relevant signals in the second hosts specifically during the effector phase after 6 dpi. We modulated Ag availability in vivo by transferring Ag-pulsed APC (Ag/APC) into second hosts or infecting second hosts 6 d previously with influenza viruses (infection-matched). Thus, we could modulate the availability of signals from infection, while normalizing cognate Ag presentation, as done later (see Fig. 5A). In experiments using the sequential transfer model, we analyzed the transferred donor effector cells 2 to 4 d posttransfer (dpt; 8 to 10 dpi) and not later because  $T_{FH}$  peak at 7 to 8 dpi (*SI Appendix, Fig. S1B*) and contract after 10 dpi.

### Cognate Ag Recognition, in the Presence of Infection at the Effector Checkpoint, Drives $T_{FH}$ Development.

We generated 6-dpi OT-II effectors in vivo as described above and transferred them into second hosts. The second hosts were either PR8-OVA<sub>II</sub> infection-matched (Ag and infection) or PR8 infection-matched (infection without Ag) or uninfected (neither infection nor Ag) (Fig. 1A). Donor  $T_{FH}$  and GC- $T_{FH}$  generation were assessed at 2 dpt in the secondary lymphoid organs (SLOs), corresponding to 8 dpi. In the PR8-OVA<sub>II</sub> infection-matched positive controls, a strong donor  $T_{FH}$  response developed in the spleen and DLN (Fig. 1B and *SI Appendix, Fig. S2B*). In contrast, in PR8 infection-matched hosts, where no cognate Ag presentation occurred, few if any donor  $T_{FH}$  were seen and donor  $T_{FH}$  numbers were reduced 25-fold in both the spleen (Fig. 1B) and the DLN (*SI Appendix, Fig. S2B*). Donor GC- $T_{FH}$  developed well in hosts with Ag and infection, while almost no GC- $T_{FH}$  were generated without Ag (Fig. 1C and *SI Appendix, Fig. S2C*). This suggests effectors have a strict requirement for Ag recognition during this phase, for development and/or maintenance of  $T_{FH}$  and GC- $T_{FH}$ . PD1 and ICOS expression, markers associated with  $T_{FH}$  function, were also strictly dependent on Ag recognition in the second host (Fig. 1D and E and *SI Appendix, Fig. S2 D and E*).

At 6 dpi, there are already a minor fraction of CD4 effectors that express the  $T_{FH}$  phenotype (CXCR5<sup>hi</sup>Bcl6<sup>hi</sup>) (*SI Appendix, Fig. S1B*), suggesting that this cohort may undergo apoptosis or revert to a non- $T_{FH}$  state in the absence of cognate Ag presentation at 6 to 8 dpi. Thus, even when signals from infection were available in the PR8-infected hosts, development of  $T_{FH}$  in the spleen and DLN required cognate Ag recognition during the effector checkpoint. A previous study showed that the transfer of 4-d effectors generated during LCMV infection into uninfected hosts did not support  $T_{FH}$  development, but it did not distinguish between the need for infection vs. Ag recognition (14). Our data indicate that even when signals from infection are available, cognate Ag at the peak effector phase is needed to drive and sustain  $T_{FH}$  and GC- $T_{FH}$  development.

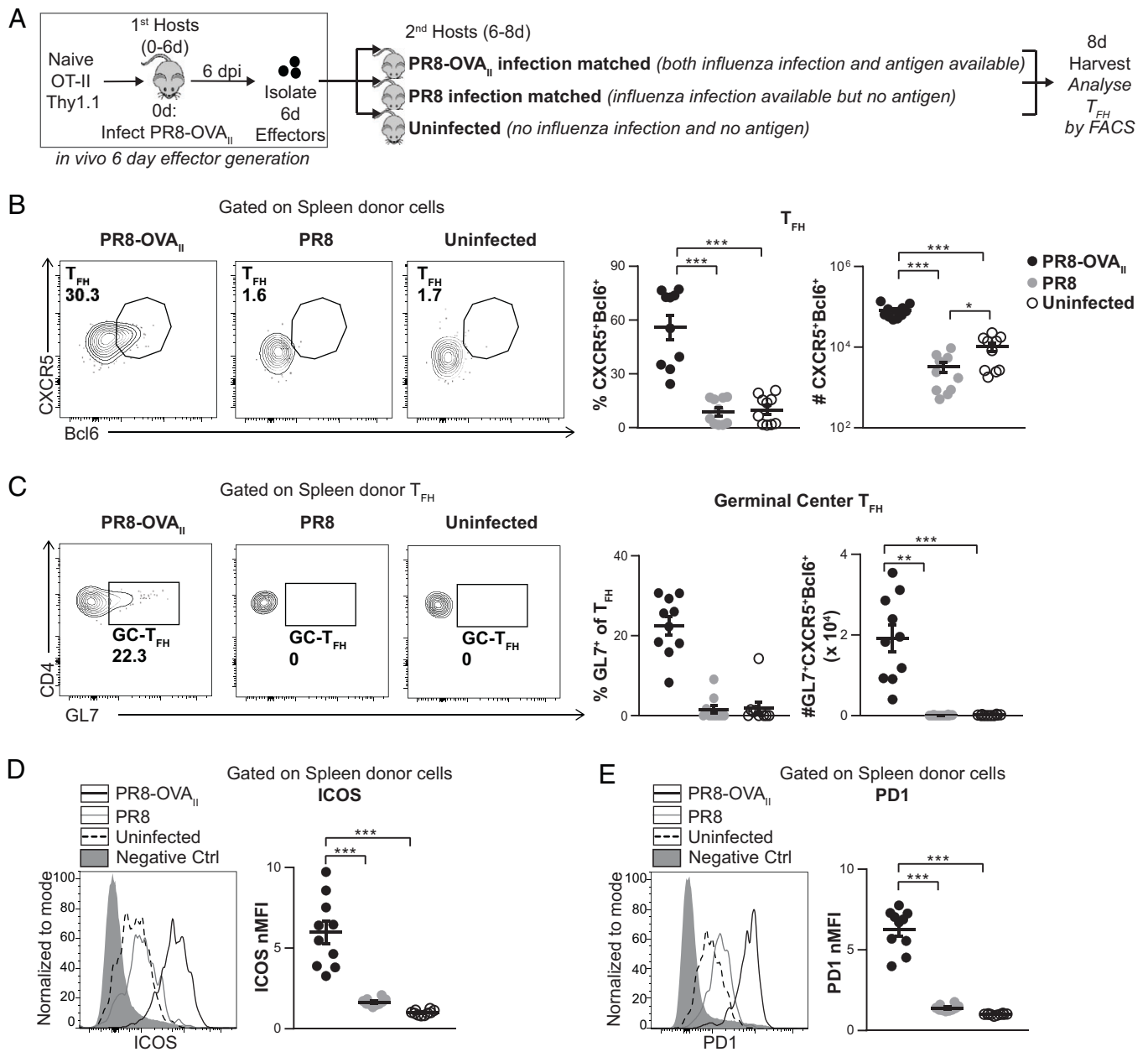


**Fig. 1.** Generation of  $T_{FH}$  from CD4 effectors requires Ag recognition during the effector checkpoint. (A) Experimental design: Naive OT-II.Thy1.1<sup>+</sup> cells were transferred into PR8-OVA<sub>II</sub>-infected mice (first hosts). At 6 dpi, OT-II.Thy1.1<sup>+</sup> effectors were isolated from first hosts and transferred into the following groups of second hosts: 6-dpi PR8-OVA<sub>II</sub>-infected, 6-dpi PR8-infected, or uninfected mice. Donor cells were analyzed 8 dpi. FACS, fluorescence-activated cell sorting. (B) Percentage and numbers of spleen donor  $T_{FH}$  (CXCR5<sup>+</sup>Bcl6<sup>+</sup>). (C) Percentage and number of spleen donor GC- $T_{FH}$  (GL7<sup>+</sup>CXCR5<sup>+</sup>Bcl6<sup>+</sup>). (D and E) Representative histogram of ICOS (D) and PD1 (E) expression by spleen donor cells (negative control: naive CD4 from uninfected mice). ICOS normalized median fluorescence intensity (nMFI) (D) and PD1 nMFI (E) expression by spleen donor cells. (A–E,  $n = 10$  per group pooled, 2 independent experiments). Error bars represent SEM. Statistical significance was determined by two-tailed, unpaired Student's  $t$  test (\* $P < 0.05$ , \*\* $P < 0.01$ , \*\*\* $P < 0.001$ ).

**$T_{FH}$  Function during Influenza Infection Is Dependent on Cognate Ag at the Effector Phase.** IL-21 produced by  $T_{FH}$  promotes  $T_{FH}$  differentiation and mediates the GC response (12). The proportion of donor effectors with the potential to secrete interleukin-21 (IL-21) was higher in second hosts with Ag than in those without Ag (Fig. 2A and *SI Appendix, Fig. S2F*). In contrast, secretion of Th1 cytokines, interferon gamma (IFN $\gamma$ ) and tumor necrosis factor alpha (TNF $\alpha$ ), was not dependent on Ag and was in fact highest in uninfected hosts (*SI Appendix, Fig. S2G*). This indicates a selective dependence of  $T_{FH}$ -associated programs, but not Th1 effector functions in the SLO, on Ag recognition during the effector checkpoint.

To evaluate the impact of Ag recognition at the effector checkpoint on the key  $T_{FH}$  function of enhancing GCB formation, we developed an *in vivo* GCB assay (Fig. 2B and *SI Appendix, Methods*). Endogenous host GCBs are undetectable from 2 to 6 dpi (*SI Appendix, Fig. S1C*), presumably because  $T_{FH}$  have not yet fully formed (*SI Appendix, Fig. S1B*). We reasoned that if functional  $T_{FH}$  were available earlier, they would accelerate GCB formation. Therefore, we transferred *in vivo*-generated 6-d OT-II effectors into hosts infected 2 d previously with either PR8 (infection only) or PR8-OVA<sub>II</sub> (infection and cognate Ag) and analyzed host GCB at 4 dpi (6 dpi) (Fig. 2B).

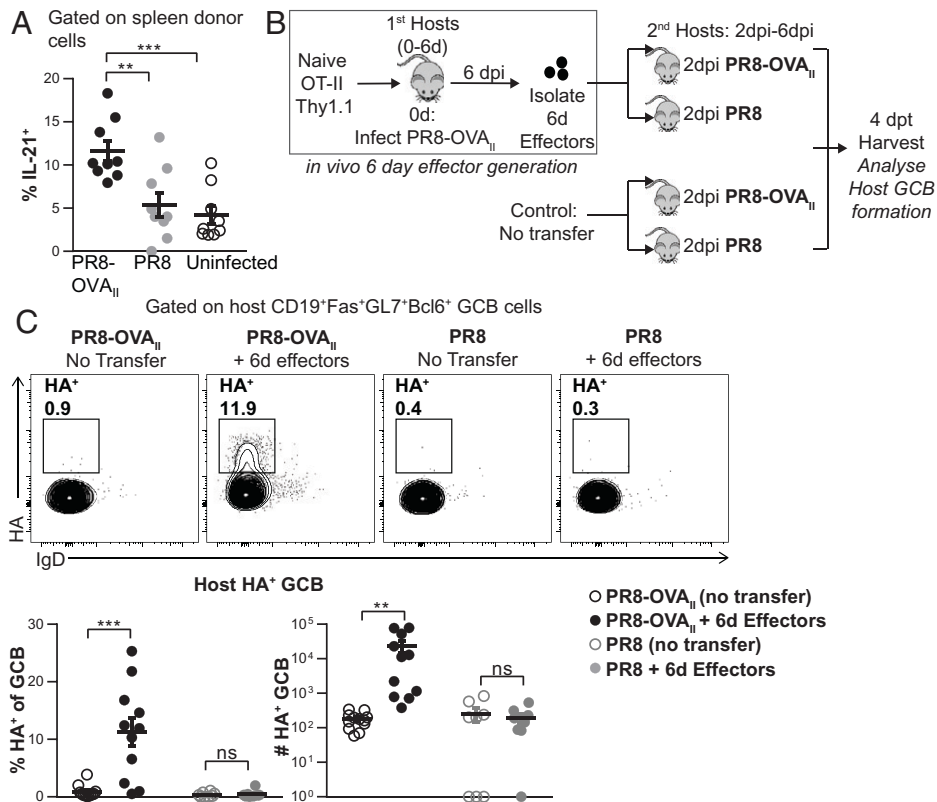


**Fig. 2.**  $T_{FH}$  function: IL-21 potential and enhanced GCB development is driven by Ag recognition during the effector phase. (A) Experiment design as in Fig. 1A. Percentage of spleen donor cells expressing intracellular IL-21 ( $n = 9$  per group pooled, 2 independent experiments). (B) Experimental design: In vivo-generated 6-d OT-II.Thy1.1<sup>+</sup> effectors were transferred into 2-dpi PR8-OVA<sub>II</sub>-infected or PR8-infected mice. Groups of 2-dpi PR8-OVA<sub>II</sub>-infected and PR8-infected mice, with no cells transferred served as negative controls. Splensins from these mice were analyzed 4 dpt. (C) Percentage and numbers of HA<sup>+</sup> GCB. ( $n = 8$  to 12 per group pooled, 2 to 3 independent experiments). Error bars represent SEM. Statistical significance was determined by two-tailed, unpaired Student's *t* test (\*\* $P < 0.01$ , \*\*\* $P < 0.001$ ; ns, not significant).

The transfer of 6-d donor effectors into PR8-OVA<sub>II</sub>-infected mice caused a significant increase in total GCB formation (*SI Appendix, Fig. S2H*) and in influenza hemagglutinin-specific GCB formation (Fig. 2C) 4 d later. Transfer of the same cells to PR8-infected hosts, which lack OVA<sub>II</sub> Ag, did not boost GCB formation over the negative controls not receiving effectors. Thus,  $T_{FH}$  induction of GCBs also requires that CD4 effectors recognize cognate Ag during the effector phase.

**Multiple APC Subsets Effectively Present Ag at the Effector Checkpoint to Drive  $T_{FH}$ .** B cells become the major APC for  $T_{FH}$  once they arrive in the follicular region of the SLO, which they repeatedly interact with for further differentiation (18). We considered the possibility that other APC subsets might be able to drive the effector to  $T_{FH}$  differentiation at 6 dpi, if and when available. We evaluated the efficacy of different broad classes of APC at presenting Ag for  $T_{FH}$  during the effector phase using B cell-deficient JhD mice, major histocompatibility complex II (MHC-II) KO bone marrow chimeras, and CD11cTg.H2-Ab1<sup>-/-</sup> mice which expressed MHC-II only on CD11c<sup>+</sup> cells, which are all second hosts. In other experiments, we provided Ag by transferring in vitro-activated, Ag-pulsed, B cells or dendritic cells (DC) (*SI Appendix, Fig. S3A*).

To determine whether Ag-presenting B cells are essential to drive CD4 effectors to  $T_{FH}$ , we transferred in vivo-generated 6-d HNT Thy1.1 (TCR Tg specific for the hemagglutinin (HA) epitope of the influenza strain) effectors into PR8 infection-matched B cell-deficient JhD mice (Fig. 3A and *SI Appendix, Fig. S3B*). Substantial numbers of  $T_{FH}$  were generated in these hosts, although there was a twofold decrease in number

compared to B cell replete hosts. This suggests that non-B cell APC can also drive  $T_{FH}$  development from effectors.

To determine what alternate endogenous APCs were competent to present Ag, we transferred 6-d effectors into infection-matched BM chimeras in which MHC-II expression was restricted to either the hematopoietic compartment (wild type [WT] → MHC-II KO chimeras) (Fig. 3B and *SI Appendix, Fig. S3C*) or to the nonhematopoietic compartment (MHC-II knock out [KO] → WT chimeras) (Fig. 3C and *SI Appendix, Fig. S3D*). Donor  $T_{FH}$  recovery was equivalent in WT mice and those with MHC-II were restricted to the hematopoietic compartment (Fig. 3B and *SI Appendix, Fig. S3C*). However, very few  $T_{FH}$  were found when Ag presentation was restricted to the nonhematopoietic compartment (Fig. 3C and *SI Appendix, Fig. S3D*), consistent with observations that few nonhematopoietic MHC-II<sup>+</sup> cells present Ag in the SLO (19).

We next transferred 6-d effectors into PR8-OVA<sub>II</sub> infection-matched CD11cTg.H2-Ab1<sup>-/-</sup> mice (Fig. 3D and *SI Appendix, Fig. S3E*). There was no defect in donor  $T_{FH}$  formation from these 6-d effectors, indicating that in infected mice, CD11c<sup>+</sup> APCs are sufficient at the effector checkpoint to drive  $T_{FH}$  development.

To compare the efficiency of DC (Fig. 3E and *SI Appendix, Fig. S3F*) and B cell (Fig. 3F and *SI Appendix, Fig. S3G*) Ag presentation, we pulsed each with Ag and transferred them with the 6-d effectors into PR8 infection-matched mice. The 6-d effectors gave rise to equivalent numbers of  $T_{FH}$  when either B cells or DC presented Ag. These experiments indicate that multiple APC types, including APCs other than B cells, are effective at driving  $T_{FH}$  development from 6-dpi effectors

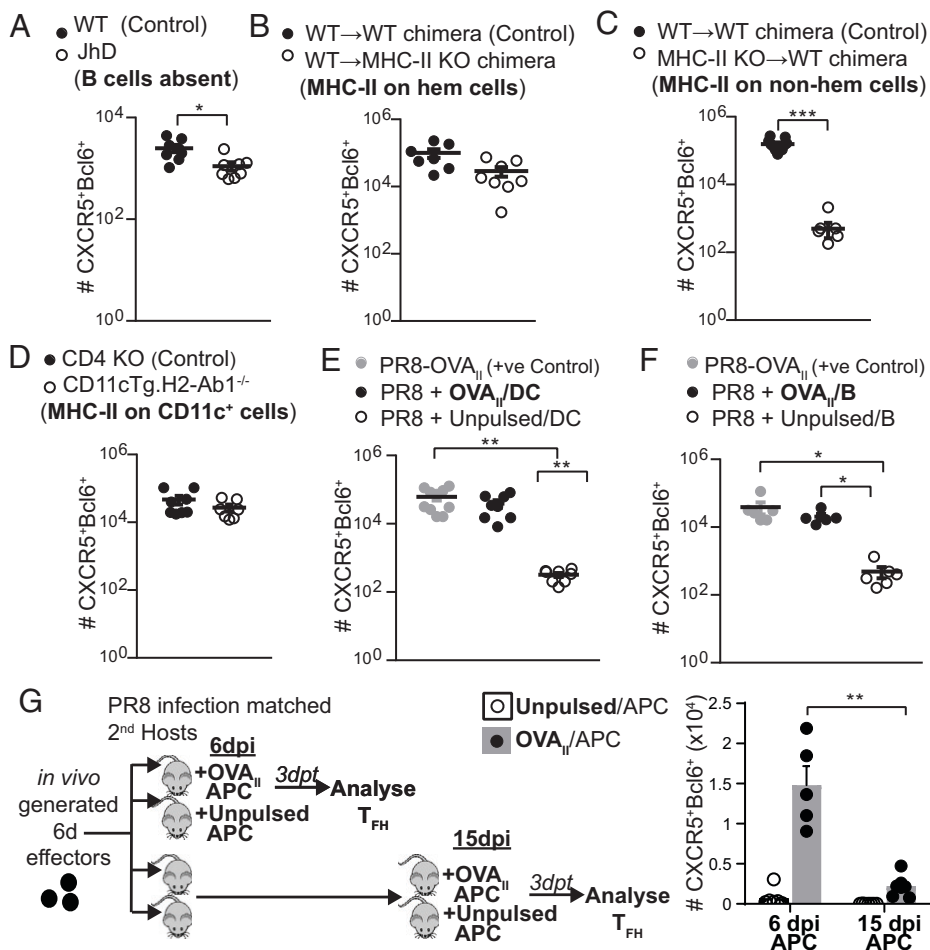


**Fig. 3.** Multiple APC subsets can present cognate Ag during the effector phase to drive T<sub>FH</sub> development from 6-d effectors. (A) Experimental design for A–F as depicted *SI Appendix, Fig. S3A* schematic: In vivo-generated 6-d OT-II.Thy1.1<sup>+</sup> or 6-d HNT.Thy1.1<sup>+</sup> effectors were transferred into PR8 infection-matched hosts (A), PR8-OVA<sub>II</sub> infection-matched hosts (B–D), or into PR8 infection-matched hosts together with OVA<sub>II</sub>/APC (E and F). Numbers of T<sub>FH</sub> (CXCR5<sup>+</sup>Bcl6<sup>+</sup>) generated were enumerated by flow cytometry, 2 to 4 dpt in each of these models. (A) JhD mice where B cells are absent or into WT control mice ( $n = 8$  per group pooled, 2 independent experiments). (B) WT→MHC-II KO (H2-Ab1<sup>-/-</sup>) bone marrow chimera mice that were made by transferring WT bone marrow into MHC-II KO irradiated hosts, where MHC-II is restricted to the hematopoietic compartment, or into WT→WT bone marrow chimera control mice ( $n = 7$  to 8 per group pooled, 3 independent experiments). (C) MHC-II KO→B6 bone marrow chimera mice, where MHC-II is restricted to the nonhematopoietic compartment or into WT→WT bone marrow chimera control mice ( $n = 8$  to 11 per group pooled, 3 independent experiments). (D) CD11cTg.H2-Ab1<sup>-/-</sup> mice where MHC-II is restricted to CD11c<sup>+</sup> cells or into CD4 KO control mice ( $n = 7$  to 11 per group pooled, 2 to 3 independent experiments). (E) WT mice with cognate Ag supplied via OVA<sub>II</sub>-pulsed BMDC vs. unpulsed BMDC controls ( $n = 8$  to 10 per group pooled, 3 independent experiments). (F) WT mice with cognate Ag supplied via OVA<sub>II</sub>-pulsed B cells vs. unpulsed B cell controls ( $n = 5$  to 6 per group pooled 2 independent experiments). (G) In vivo-generated 6-d OT-II.Thy1.1<sup>+</sup> were transferred into PR8 infection-matched hosts. OVA<sub>II</sub>/APCs were transferred either on 6 d along with the effectors or on 15 d. Numbers of T<sub>FH</sub> (CXCR5<sup>+</sup>Bcl6<sup>+</sup>) generated were enumerated by flow cytometry, 3 dpt. For OVA<sub>II</sub>/APCs, we used in vitro-stimulated T-depleted splenocytes that contained a mixture of APC types, predominantly B cells, since we had determined the kind of APC was not important ( $n = 5$  to 6 per group pooled 2 independent experiments). Error bars represent SEM. Statistical significance determined by two-tailed, unpaired Student's *t* test (\* $P < 0.05$ , \*\* $P < 0.01$ , and \*\*\* $P < 0.001$ ).

during influenza infection, as long as hematopoietic MHC-II<sup>+</sup> presentation is available.

T<sub>FH</sub> begin to differentiate within the first few rounds of CD4 division (20), and thus, 6-d effectors contain partially differentiated pre-T<sub>FH</sub> effectors. It is possible that these pre-T<sub>FH</sub> can persist in the absence of signals from cognate Ag during the effector phase and are ready to develop into T<sub>FH</sub> later, if cognate-Ag becomes available. To evaluate this possibility, we transferred 6-d OT-II effectors into PR8 infection-matched hosts (Fig. 3G), so other signals from infection and GC responses were available, but cognate-Ag was not. As a positive control, we transferred OVA<sub>II</sub>/APC at 6 dpi. T<sub>FH</sub> developed from 6-d effectors when they were transferred together with OVA<sub>II</sub>/APC, as in Fig. 3E and F. However, when we delayed the transfer of OVA<sub>II</sub>/APC to 15 dpi, sixfold to sevenfold fewer T<sub>FH</sub> were generated from the transferred 6-d effectors (Fig. 3G). This

mirrored the contraction of total CD4 effectors, whose numbers were also reduced sevenfold to eightfold when the addition of OVA<sub>II</sub>/APC was delayed to 15 dpi (*SI Appendix, Fig. S3H*). This suggests that pre-T<sub>FH</sub> effectors undergo contraction in the absence of cognate Ag after 6 dpi. Thus, continuing Ag presentation through this effector checkpoint is essential for the 6-d effectors to avoid contraction and complete their differentiation into T<sub>FH</sub>, even if they receive the early signals and even if other signals from infection and from the GC are available.

**Ag Delivery by Different Routes Favors Ag Presentation in Distinct Sites and Selectively Drives T<sub>FH</sub> in DLN vs. Spleen.** T<sub>FH</sub> are restricted to the SLO (DLN and spleen) during primary infection and express signatures for residency in SLO (21–23). In the influenza model, we do not find T<sub>FH</sub> in the lung during the primary effector response, although they are found during the

memory phase after 14 dpi and during secondary effector responses in the lung (24). To design vaccine delivery strategies that mimic the superior protection elicited after infection, we needed to understand if the site of Ag presentation during the effector phase plays a role in  $T_{FH}$  generation.

We followed Ag/APC after different routes of transfer and evaluated where the CD4 effector interaction with Ag/APC needed to occur for  $T_{FH}$  to develop in the spleen vs. the DLN (Fig. 4A). We transferred OT-II.Nur77<sup>GFP</sup>.Thy1.1<sup>+</sup> 6-d effectors into PR8 infection-matched hosts with the OVA<sub>II</sub>/APC introduced by different routes and analyzed them 14 to 16 h post-transfer (Fig. 4B and C). OVA<sub>II</sub>/APCs were found in the lung only after intranasal (i.n.) transfer and in the spleen only after intrasplenic (i.s.) transfer (Fig. 4B). Next, we examined Ag presentation as indicated by Nur77 expression in the transferred OT-II in the different sites. Transfer of OVA<sub>II</sub>/APC i.n. induced Nur77<sup>GFP</sup> expression in the DLN, and not in the spleen, while i.s. transfer induced Nur77<sup>GFP</sup> exclusively in donor cells recovered from the spleen and not in the DLN (Fig. 4C), indicating we had achieved localized Ag presentation.

We found the total number of donor cells recovered in the DLN increased following i.n. but not i.s. OVA<sub>II</sub>/APC transfer and vice versa; the number of donor cells recovered in the spleen was increased following i.s. but not i.n. OVA<sub>II</sub>/APC transfer (Fig. 4D). In parallel,  $T_{FH}$  developed from donor cells in the DLN only when OVA<sub>II</sub>/APCs were administered by the i.n. and not i.s. route (Fig. 4E and *SI Appendix, Fig. S4A*) and in the spleen only when OVA<sub>II</sub>/APCs were delivered by the i.s. and not i.n. route (Fig. 4F and *SI Appendix, Fig. S4A*). Thus,  $T_{FH}$  development correlated with the location of Ag/APCs and with Ag presentation to the CD4 T cells. This implies that full  $T_{FH}$  development requires that the CD4 effectors recognize Ag in the tissue in which they become resident, indicating local Ag presentation is needed.

We also tested if Ag/APCs delivered intravenously (i.v.) might result in presentation to CD4 effectors before they reached their SLO sites and would be sufficient to complete their differentiation into  $T_{FH}$ . We i.v. transferred OVA<sub>II</sub>/APC with OT-II.Nur77<sup>GFP</sup>.Thy1.1<sup>+</sup> 6-d effectors. After 14 to 16 h, donor effectors in both the spleen and DLN expressed Nur77<sup>GFP</sup>, indicating Ag recognition (Fig. 4G). However, after i.v. transfer, the APCs were found predominantly in the spleen with many fewer in the lung (Fig. 4H). OVA<sub>II</sub>/APCs transfer by the i.v. route, like transfer by i.n., increased the number of transferred effectors in the DLN, compared to the negative control (Fig. 4I). However, OVA<sub>II</sub>/APCs transferred i.v. supported donor spleen  $T_{FH}$  but not DLN  $T_{FH}$  generation (Fig. 4J and K and *SI Appendix, Fig. S4B and C*). This suggests that even if 6-d effectors have the opportunity to recognize Ag before migrating to their site of residence in the DLN (as here during i.v. transfer), this is not sufficient to induce the development of  $T_{FH}$  in DLN because they require Ag recognition targeted to the specific SLO. These results emphasize that while many APCs may effectively present Ag, it is essential that during this effector checkpoint, the Ag is optimally delivered to the organ where the  $T_{FH}$  will develop.

**Signals from Infection during the Effector Phase Are Required to Support  $T_{FH}$ .** Infection-generated signals activate APCs, but they also induce innate pathways that produce inflammatory signals independent of cognate Ag presentation (25). We reasoned that during influenza infection, abundant pathogen recognition signals continue through the effector checkpoint due to the continuing presence of live, replicating virus (6). The impact of Ag-independent signals from influenza infection during the effector checkpoint can be analyzed by normalizing cognate Ag presentation to CD4 effectors, using Ag/APC as the sole source of Ag (Fig. 5A). We transferred in vivo-generated 6-d OT-

II.Nur77<sup>GFP</sup>.Thy1.1<sup>+</sup> effectors along with OVA<sub>II</sub>/B cell APCs into IAV infection-matched or uninfected second hosts (Fig. 5A). After 14 to 16 h (*SI Appendix, Fig. S5A*), there was no significant difference in the number of transferred APCs or in Nur77<sup>GFP</sup> expression by the donor effectors in infected and uninfected mice, indicating that the transferred APCs present Ag equivalently in both hosts. Thus, the only variable was the presence of signals from influenza infection unrelated to Ag presentation. We found that the proportion of donor  $T_{FH}$  at 3 to 4 dpt in the spleen of uninfected second hosts was lower than that in IAV-infected hosts (Fig. 5B). We analyzed the expression of signature proteins associated with  $T_{FH}$  function and found that donor  $T_{FH}$  in infected mice also expressed significantly higher levels of Bcl6, PD1, and ICOS (Fig. 5C and D and *SI Appendix, Fig. S5C*) than in uninfected mice.

To additionally evaluate Ag-independent effects of infection, we used influenza B virus (IBV) infection (Fig. 5E and *SI Appendix, Fig. S5D–J*). IBV has little homology with IAV (26).  $T_{FH}$  and GC- $T_{FH}$  generation from transferred 6-d effectors in IBV-infected mice were higher than those in uninfected mice, with higher Bcl6 and ICOS expression, confirming a contribution of infection, independent of Ag presentation (*SI Appendix, Fig. S5D–G*). We repeated the experiment using DC instead of B cells as the source of OVA<sub>II</sub>/APC to normalize Ag presentation (Fig. 5E and *SI Appendix, Fig. S5H–J*) and found a similar dependence of  $T_{FH}$  and GC- $T_{FH}$  generation on infection. The data indicate that optimum  $T_{FH}$  development requires signals generated by infection at the effector checkpoint, which are independent from and in addition to signals from cognate Ag recognition.

### In a Polyclonal Vaccine Model, Providing Both Ag and Infection Signals at the Effector Checkpoint Induces Strong $T_{FH}$ Responses Comparable to Influenza Infection.

Our results indicate that optimal  $T_{FH}$  development requires both Ag recognition and infection signals during the effector checkpoint. We postulate that when conventional vaccines do not provide these signals, they induce much less  $T_{FH}$  than live infection. To explore this hypothesis in an in situ polyclonal response, we developed a model using the following two widely used vaccine approaches: nonreplicating inactivated influenza vaccine (IIV) and live attenuated influenza vaccine (LAIV) (27). We showed that IIV provides high-level Ag presentation only transiently (8) (*SI Appendix, Fig. S1A*). LAIV contains attenuated influenza viruses that are cold adapted, so replication is restricted to the upper respiratory tract and does not occur in the warmer lung environment (27). Since LAIV contains live replication-competent virus, it is likely to provide stronger infection signals than IIV. We treated mice with two doses of IIV (8) or LAIV (7) at d 0 and at d 6 to supply Ag presentation and signals from infection, for both priming and through the checkpoint (Fig. 6A). We compared the vaccine responses to the infection-generated  $T_{FH}$  response. Virus-specific T cells were detected by tetramer staining for an immunodominant epitope in B6 mice, NP<sub>311</sub>.

Adding a second dose of either vaccine at the effector checkpoint increased the total number of NP<sub>311</sub> tetramer<sup>+</sup> cells by threefold over just one dose (Fig. 6B). Both the number of NP<sub>311</sub> tetramer<sup>+</sup> cells (Fig. 6B) and the number of GCB cells (*SI Appendix, Fig. S6A*), following a second dose of either vaccine at the checkpoint, were comparable to those generated during influenza infection. Two doses of LAIV resulted in a fourfold increase in the proportion of  $T_{FH}$  compared to one dose, resulting in a higher proportion of  $T_{FH}$  generation than during influenza infection (Fig. 6C and D). Moreover, with two doses of LAIV, an equivalent number of  $T_{FH}$  were generated as following influenza infection (Fig. 6D) which was over 10-fold higher than that with just one dose of LAIV at d 0. In contrast,

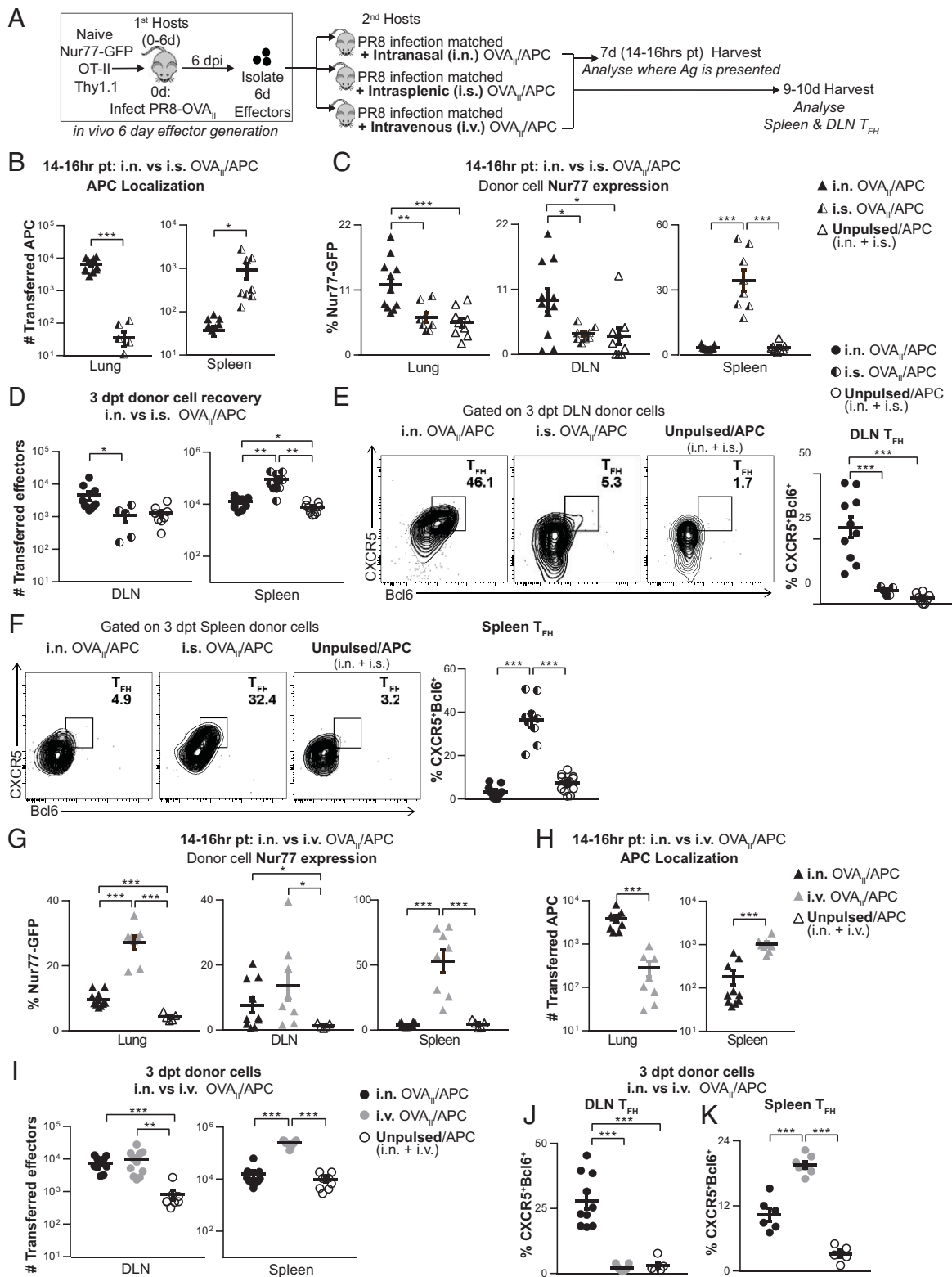


**Fig. 4.** Local Ag presentation during the effector phase is required for DLN and spleen T<sub>FH</sub> as shown by Ag delivery via i.n. vs. i.s. vs. i.v. routes. (A) Experimental design: OVA<sub>II</sub> peptide-pulsed B cells (CD45.1<sup>+</sup> or GFP<sup>+</sup>) were used as APCs and transferred into PR8 infection-matched hosts 6 dpi by either i.n., i.s., or i.v. routes. Unpulsed APCs were transferred both i.n. and i.s., or both i.n. and i.v., as negative controls. In vivo-generated 6-d OT-II.Nur77<sup>GFP</sup>.Thy1.1<sup>+</sup> effectors were transferred by i.v. route. Mice were harvested 14 to 16 h posttransfer (pt), and donor cells were analyzed by flow cytometry. (B and H) Number of transferred APCs. (C and G) Donor cell Nur77<sup>GFP</sup> expression was analyzed by flow cytometry in the lung, DLN, and spleen. (n = 8 to 11 per group pooled, 3 independent experiments). (D–F, I, and J) Experiment was performed as in A, and mice were euthanized 3 to 4 dpt. (D and I) Total numbers of DLN and spleen donor effectors recovered (n = 5 to 12 per group pooled, 3 to 4 independent experiments). (E and J) DLN T<sub>FH</sub> formation from donor cells (n = 5 to 11 per group pooled, 2 to 3 independent experiments) (F and K) Spleen T<sub>FH</sub> formation from donor cells (n = 5 to 12 per group pooled, 2 to 4 independent experiments).

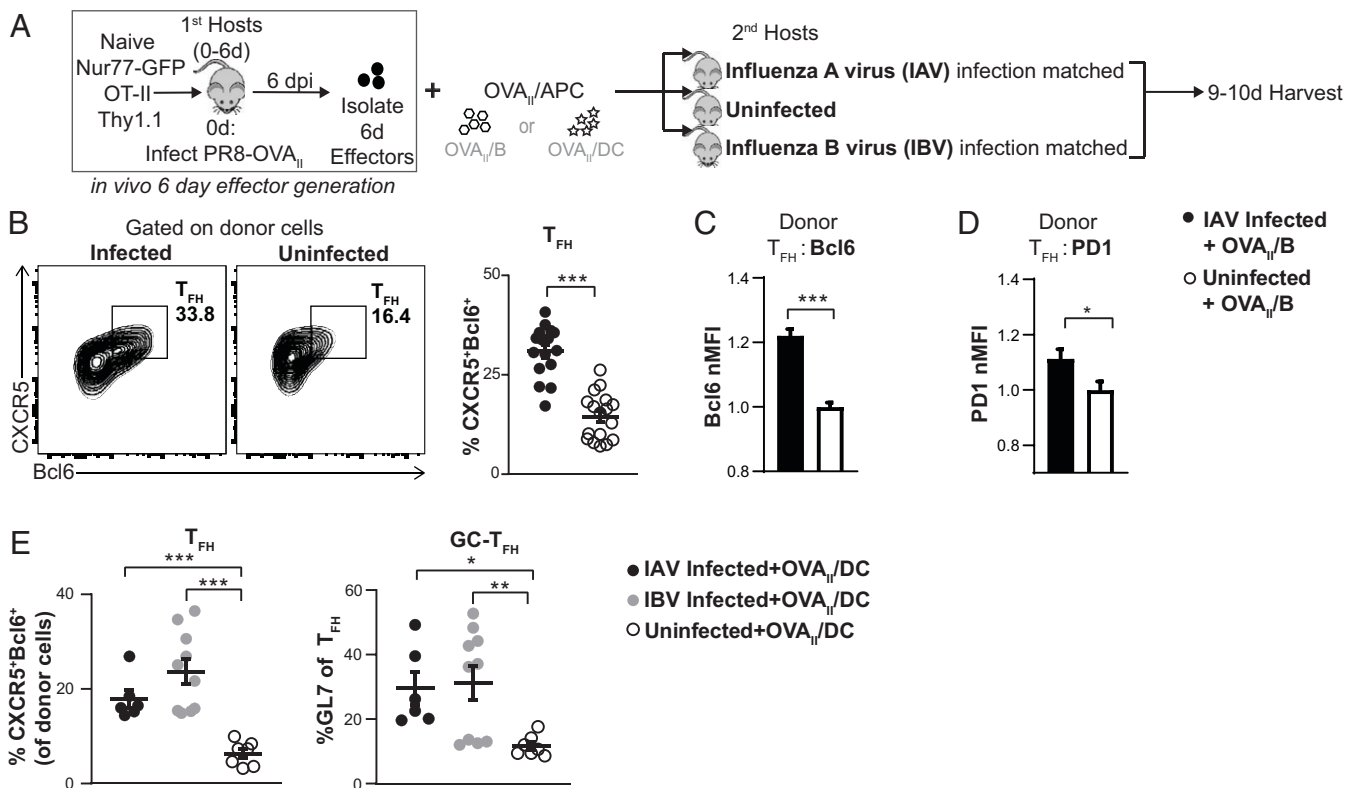


**Fig. 5.** Ag independent signals from infection support T<sub>FH</sub> during the effector checkpoint. (A) Experimental design: In vivo-generated 6-d OT-II.Nur77<sup>GFP</sup>.Thy1.1<sup>+</sup> effectors were transferred i.v. along with OVA<sub>II</sub> peptide-pulsed B cells (B–D) or OVA<sub>II</sub> peptide-pulsed DC (E) that were transferred both i.n. and i.v. into second hosts that were either infection-matched with IAV (PR8) or with IBV (B/Ann Arbor/1/66) or that were uninfected. (B–D) The 6-d effectors + OVA<sub>II</sub>/B were transferred into IAV infection-matched vs. uninfected hosts, 3 to 4 dpi. Splens were analyzed by FACS for T<sub>FH</sub> generation from donor cells (B), Bcl6 normalized MFI of the T<sub>FH</sub> (C), and PD1 normalized MFI of the T<sub>FH</sub> (D). (B–D)  $n = 16$  to 17 per group pooled from 5 independent experiments. (E) The 6-d effectors + OVA<sub>II</sub>/DC were transferred into IAV or IBV infection-matched or uninfected hosts, 4 dpi. Splens were analyzed by FACS for T<sub>FH</sub> generation from donor cells.  $n = 6$  to 10 per group pooled from 2 independent experiments. Error bars represent SEM. Statistical significance was determined by two-tailed, unpaired Student's  $t$  test (\* $P < 0.05$ , \*\* $P < 0.01$  and \*\*\* $P < 0.001$ ).

the second dose of IIV did not increase the proportion of T<sub>FH</sub> generation over one dose (Fig. 6 C and D), even though the number of total NP<sub>311</sub><sup>+</sup> CD4 effectors generated were equivalent to those of a live infection (Fig. 6B). A similar effect on T<sub>FH</sub> generation was seen when analyzing the total polyclonal CD4 response (SI Appendix, Fig. S6B). Strikingly, the impact of adding a checkpoint dose of LAIV in inducing GC-T<sub>FH</sub> generation was even more pronounced. Two doses of LAIV induced 20-fold more GC-T<sub>FH</sub> than one dose and was equivalent to the levels induced by infection, while two doses of IIV did not induce levels equivalent to infection (Fig. 6E). Two doses of LAIV were also able to induce Bcl6 and PD1 expression in T<sub>FH</sub> to levels comparable to infection, but two doses of IIV did not (Fig. 6 F and G).

T<sub>FH</sub> are essential to induce IgG1 Ab in models of influenza immunization, while Th1 effectors are sufficient to induce IgG2 Ab (28). In line with those findings, two doses of LAIV induced IgG1 plasmablasts equivalent to those found after influenza infection, while two doses of IIV were unable to do so (Fig. 6H), thus mimicking T<sub>FH</sub> induction in Fig. 6D. Both IgG2c and IgG2b plasmablasts were induced by two doses of LAIV, as well as two doses of IIV (Fig. 6 I and J). This is expected since both strategies induced equivalent CD4 effector expansion (Fig. 6B). Similar patterns were also seen in levels of IgG1 and IgG2 serum Ab 1 mo after immunization (Fig. 6 K–M and SI Appendix, Fig. S6 C–E), with two doses of LAIV inducing enhanced IgG1 levels compared to one dose, while two doses of IIV did not induce more IgG1 than one dose (Fig. 6K). Two

doses of LAIV and IIV were both able to induce enhanced IgG2c and IgG2b compared to one dose (Fig. 6 L and M). Several comprehensive B cell studies have also shown that T<sub>FH</sub> are critical for the increased potency of Ab generated (such as neutralizing ability, increased mutation diversity, increased affinity, increased avidity) and correlate with memory B cell responses that confer stronger protection against infection (20, 28). Our findings here indicate that the requirements established in a reductionist monoclonal TCR Tg transfer model translate readily to a vaccine model in which in situ polyclonal responses are analyzed. This supports the concept that it should be possible to achieve T<sub>FH</sub>-driven immunity nearly comparable to influenza infection by using vaccines that supply optimal Ag and infection signals during the checkpoint, in addition to during priming.

## Discussion

Influenza infection generates long-lived Ab responses that provide much stronger protection against reinfection than current influenza vaccines (5). We interrogated aspects of live influenza infection that generate strong protection to provide insights into designing more effective vaccines. We identified the following three key mechanisms during the CD4 effector phase of an influenza infection that together drive full T<sub>FH</sub> development: sustained Ag presentation through the effector phase, Ag presentation in the site of T<sub>FH</sub> residence, and the presence of ongoing infection. We confirmed the relevance of these observations in a vaccine setting by showing that a double vaccination with LAIV at d 0 and d 6 induced the generation of high

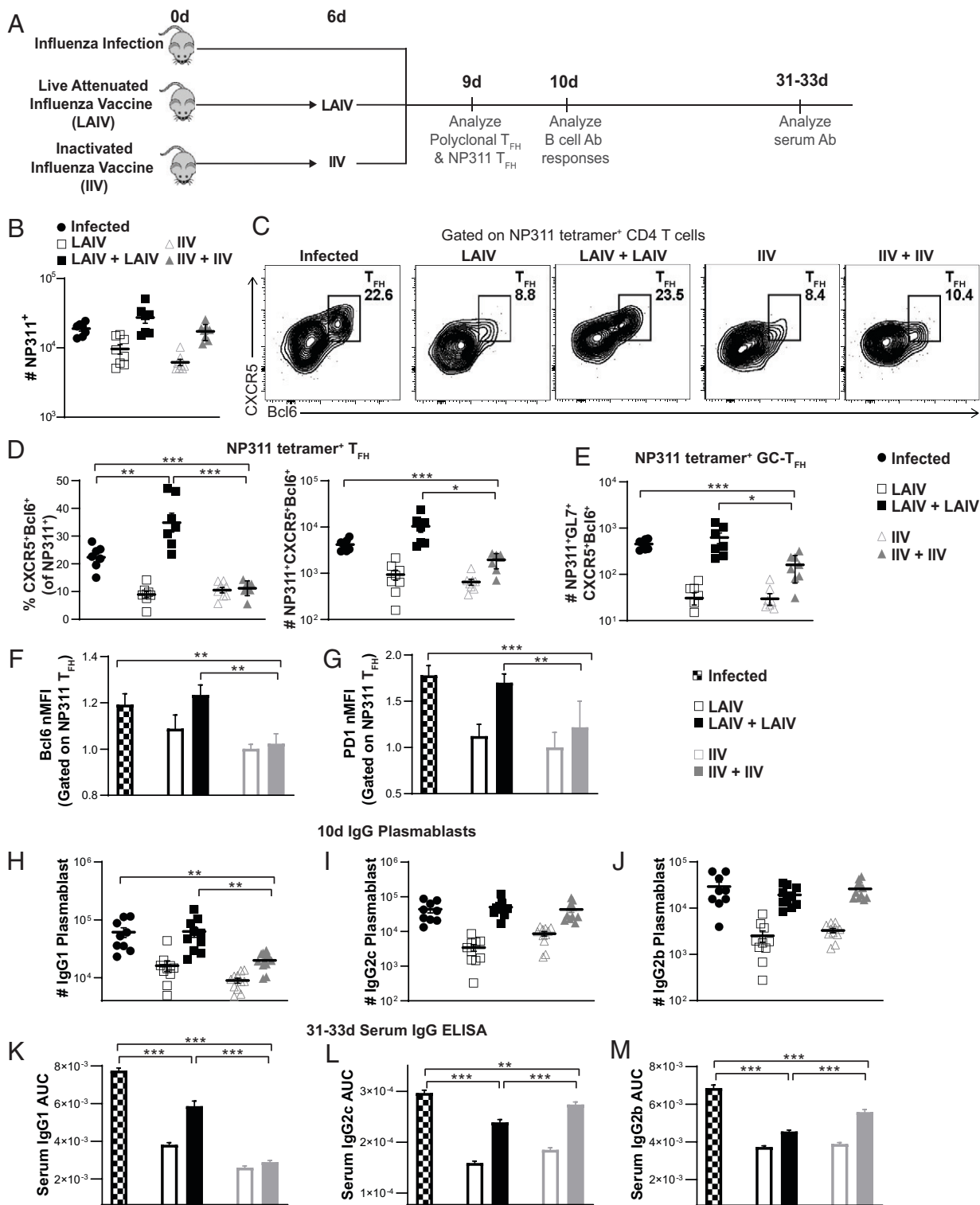


**Fig. 6.** Live attenuated influenza immunization that supplies both Ag and signals from infection at the effector checkpoint supports T<sub>FH</sub> generation, IgG plasmablast formation, and serum IgG levels near those of natural influenza infection. (A) Experimental design: One group of mice were infected with IAV. Two groups of mice were either given one dose of LAIV on d 0 or two doses on d 0 and d 6. Two groups of mice were either given one dose of IIV on d 0 or two doses on d 0 and d 6. Mice were euthanized at 9 d, 10 d or 31–33 d after infection/initial immunization. Virus-specific responses in the spleen were analyzed by staining with NP311 tetramer. (B) Total number of NP311<sup>+</sup> CD4 T cells. (C and D) T<sub>FH</sub> generation by NP311<sup>+</sup> CD4 T cells. (E) GC-T<sub>FH</sub> generation by NP311<sup>+</sup> CD4 T cells. (F and G) Normalized MFI of Bcl6 (F) and PD1 expression (G) by NP311<sup>+</sup> T<sub>FH</sub> cells. (B–G) *n* = 7 to 8 per group pooled from 2 independent experiments. (H–J) IgG plasmablast generation in the spleen at 10 d was analyzed by FACS staining for IgG1<sup>+</sup>CD138<sup>+</sup>CD19<sup>+</sup>IgD<sup>−</sup>GL7<sup>−</sup> (H), IgG2c<sup>+</sup>CD138<sup>+</sup>CD19<sup>+</sup>IgD<sup>−</sup>GL7<sup>−</sup> (I), and IgG2b<sup>+</sup>CD138<sup>+</sup>CD19<sup>+</sup>IgD<sup>−</sup>GL7<sup>−</sup> (J). *n* = 9 to 11 per group pooled from 3 independent experiments. Statistical significance was determined by two-tailed, unpaired Student's *t* test. (K–M) IgG serum Ab was analyzed by ELISA at 31 to 33 d. Area under the curve (AUC) analyses shown that were performed for IgG1 (K), IgG2c (L), and IgG2b (M) ELISA curves are in *SI Appendix, Fig. S5 C–E*. *n* = 8 per group pooled from 2 independent experiments. Statistical significance was determined by one-way ANOVA. Error bars represent SEM. (\**P* < 0.05, \*\**P* < 0.01 and \*\*\**P* < 0.001).

levels of  $T_{FH}$  and GC- $T_{FH}$  comparable to those achieved by influenza infection.

We postulate that these requirements for effector differentiation provide a checkpoint mechanism that limits  $T_{FH}$  generation and high affinity Ab to those situations where there is an ongoing threat from continuing infection. This should limit unnecessary, potentially harmful  $T_{FH}$  responses, when they are not required for pathogen clearance. Indeed, in certain autoimmune diseases and chronic infections during which continuous Ag and inflammation persist, exaggerated  $T_{FH}$  responses lead to exaggerated humoral responses (29, 30). When viral and likely other pathogens, persist at the effector phase of the response, it suggests that the early arms of the immune response have failed to clear virus, indicating a strong infection that warrants the development of immune memory (both CD4 memory [7, 17] and Ab production helped by  $T_{FH}$ ) for future protection. Thus, the checkpoint determines the generation of much of the long-term protection against future infections.

During polyclonal responses, new naive CD4 T cells are recruited throughout the response (6) and individual polyclonal cells have different propensities to become  $T_{FH}$  because they express different TCRs (18). We circumvented these confounding factors by using TCR Tg CD4 T cells that give a more synchronized effector response. It also allowed us to use a sequential transfer model to study effector phase signals specifically after the 6-dpi timepoint.

In influenza-infected mice, 6 dpi marks the beginning of GC formation (31) (*SI Appendix, Fig. S1 B and C*). It also coincides with the checkpoint for CD4 memory, when CD4 effectors require Ag recognition to induce IL-2 production, which blocks apoptosis and initiates transition to memory (7, 17). The substantial diminution of  $T_{FH}$ , when cognate-Ag presentation is absent from 6 to 15 d (Fig. 3G), suggests that Ag recognition also prevents the default contraction of the pre- $T_{FH}$  CD4 effectors, while inducing further  $T_{FH}$  differentiation. Until recently, it was thought that  $T_{FH}$  are largely quiescent during this time, but our results here and a recent study (16) indicate that  $T_{FH}$  actively divide and are dynamically regulated during this phase.

Developing  $T_{FH}$  requires repeated Ag recognition and costimulatory interactions once they reach the T-B border in the GC of the SLO (18), which are presumed to occur during their cognate interaction with GCBs. Thus, it was assumed that further differentiation of  $T_{FH}$  including their development into GC- $T_{FH}$  depended on Ag recognition during the GC response. Indeed, it has recently been shown that already generated GC- $T_{FH}$  get selected for high affinity in the GC (16). It has been unclear if signals from viral infection are needed at this stage. In previous studies that provided evidence that infection during the effector phase contributes to  $T_{FH}$  generation, it was not clear whether infection acted by supplying cognate Ag and/or by induction of infection-induced pathogen recognition signals (14). We find that at this pre-GC checkpoint, the requirement for infection after 6 dpi provides Ag-independent infection-derived signals, which must act together with Ag recognition to fully drive  $T_{FH}$  and GC- $T_{FH}$  differentiation. The frequency of  $T_{FH}$ , including GC- $T_{FH}$ , were enhanced when infection signals were present (Fig. 5).  $T_{FH}$  generated in the absence of infection expressed lower levels of Bcl6, PD1, and ICOS. Bcl6<sup>low</sup>  $T_{FH}$  rapidly lose proliferative potential and gradually gain migratory potential for egress from the LN (32). PD1 and ICOS control  $T_{FH}$  tissue positioning, and if their expression is reduced in  $T_{FH}$ , there is a breakdown of  $T_{FH}$  and GC responses (33, 34). Our results complement recent research which shows that signals from bacterial infection can augment  $T_{FH}$  (35).

The evidence that various activated MHC-II<sup>+</sup> APCs, including DC and B cells, are able to drive donor effectors to develop into  $T_{FH}$  (Fig. 3) is consistent with previous studies of APC subsets required during initial priming of  $T_{FH}$  responses (13,

36, 37). Strikingly,  $T_{FH}$  were generated from 6-d effectors even when Ag was presented only by DC (Fig. 3E and *SI Appendix, Fig. S3F*) and even in the absence of B cells and GC in JhD second hosts (Fig. 3A and *SI Appendix, Fig. S3B*). Thus, although B cells may be the major source of Ag for  $T_{FH}$  once they enter GC in situ, other MHC-II<sup>+</sup> APCs are sufficient to drive  $T_{FH}$  development at the effector phase. Given the critical importance of  $T_{FH}$ , this may allow the development of strong  $T_{FH}$  responses even when GC responses are impaired or Ag-specific B cells are limited. This may be a useful strategy for the immune system to drive GC-independent B cell responses which benefit from  $T_{FH}$  help, such as reactivation of previously generated memory B cells.

Aspects of the  $T_{FH}$  developmental program are expressed early during CD4 effector activation when effectors begin to express Bcl6 within the first few rounds of cell division (12). Thus, the 6-d effectors we transfer include some pre- $T_{FH}$  at 6 dpi before the GC phase has begun (*SI Appendix, Fig. S1 B and C*). These 6-d pre- $T_{FH}$  likely have the potential to become  $T_{FH}$  and GC- $T_{FH}$ , but our data here (25-fold reduction to negligible  $T_{FH}$  levels in the absence of Ag) suggest they contract and fail to realize that potential unless they receive local signals from Ag recognition and infection again during the effector phase.

We were able to restrict Ag presentation to distinct sites by introducing the Ag-pulsed APCs by different routes (Fig. 4). Development of the SLO-resident  $T_{FH}$  subsets require local Ag presentation in the tissue to which they will be restricted during the effector phase (Fig. 4 B-F), even if they also encountered Ag before entering the tissue (Fig. 4 G-J). This local Ag requirement is akin to that of T and B resident memory subsets that reside in nonlymphoid tissues (38-41).  $T_{FH}$  in the SLO express universal tissue residency programs (22, 23), raising the possibility that the local Ag requirement may be necessary for inducing local residency. The transferred Ag-pulsed B cells introduced here by different routes localized dependably in tissues, but it is likely that soluble protein Ag in vaccines injected intramuscularly may become distributed more systemically. Further studies are needed to determine how routes of immunization impact the locations of Ag presentation. Given the critical functions of  $T_{FH}$  that develop in the SLO, the need for local Ag presentation at the effector stage is likely important to consider during vaccine design.

$T_{FH}$  generation is a reliable indicator of protective Ab after influenza vaccination (2). Thus, vaccines that confer long-term effective Ab-mediated protection must, like natural influenza infection, provide the signals described here for pre-GC 6-d  $T_{FH}$  to fully develop into  $T_{FH}$  and GC- $T_{FH}$ . We note that mRNA lipid nanoparticle (LNP) vaccines, such as current mRNA COVID-19 vaccines, are highly effective against SARS-CoV-2 infection. These mRNA vaccines induce Ag production for an extended duration (42), and the LNPs are inflammatory (43) which may allow them to present Ag and provide inflammatory cues through the effector checkpoint and thus robustly induce  $T_{FH}$ .

Unformulated soluble Ag/adjuvants in vaccines are rapidly cleared from the body (44), which may explain the low efficacy of several current, widely used influenza vaccines. Recent studies have supported the concept that vaccine design that allows for the sustained delivery of Ag, thus mimicking Ag presentation during natural infections, results in stronger immune responses (45). Several vaccine formulation strategies have been proposed to extend the kinetics of Ag presentation (44). An extended delivery approach using osmotic pumps or escalating dose delivery resulted in superior Ab responses to HIV vaccination (46). A microneedle patch that allowed for sustained Ag delivery over 2 wk also enhanced GC,  $T_{FH}$ , and Ab responses (47). A hydrogel formulation that extended Ag delivery and supplied pathogen recognition receptor (PRR) signals

resulted in similar increases in Ab titers, specifically IgG1 correlating to the induction of  $T_{FH}$  (48). Our data suggest that extended delivery vaccines provide enhanced protection due to their induction of superior  $T_{FH}$  responses by presenting Ag through the effector phase. We also find that an additional aspect, namely, signals from infection that are independent of cognate Ag, also play an important role in the robust  $T_{FH}$  response seen during influenza infection. One way of supplying these signals is to use live attenuated vaccines. Here, we found that a vaccine regimen supplying Ag and infection signals, at priming and again at the effector checkpoint, could convert a weak response to conventional vaccination, which induced no  $T_{FH}$  to a  $T_{FH}$  response comparable to infection (Fig. 6). A second dose of IIV provided at the checkpoint was insufficient to induce  $T_{FH}$  at comparable levels to live infection and did not induce IgG1 Ab, which is known to require  $T_{FH}$  help (28). In contrast, two doses of LAIV, which uses cold-adapted influenza viruses as does the Flumist vaccine, induced  $T_{FH}$  as well as IgG1 and IgG2 plasmablasts comparable to influenza infection. In humans, LAIV has been shown to induce broader and more long-lived Ab responses in contrast to inactivated vaccines that are provided intramuscularly and do not provide signals from infection (5).

Insights from our study of mechanisms driving robust  $T_{FH}$  during influenza infection are also likely applicable to vaccine design for other infectious diseases. Our results suggest that an ideal universal influenza vaccine must, like natural IAV infection, provide the effector phase signals identified here at the right time and in the relevant sites, in order to drive an effective and durable anti-influenza response which is dependent on robust  $T_{FH}$  and GC- $T_{FH}$  (27).

## Materials and Methods

**Mice.** C57BL/6J (B6), B6.CD45.1, B6.Thy1.1, B6.Nr4a1<sup>eGFP</sup> (Nur77<sup>GFP</sup>), and B6.MHC-II<sup>-</sup> were obtained from the Jackson Laboratory. Y-linked B6.OT-II mice were obtained from Dr. Linda Bradley and were originally published by Dr. Frank Carbone's group (49); JhD mice were obtained from Dr. Mark Shlomchik; CD11cTg.H2-Ab1<sup>-/-</sup> mice were obtained from Dr. Terri Lauffer; BALB/c.HNT were obtained from Dr. David Lo (50), and these strains were bred and maintained at the UMMS animal facility. Mice were at least 8 wk old prior to use.

1. S. Crotty, T follicular helper cell biology: A decade of discovery and diseases. *Immunity* **50**, 1132–1148 (2019).
2. M. Koutsakos, T. H. O. Nguyen, K. Kedzierska, With a little help from T follicular helper friends: Humoral immunity to influenza vaccination. *J. Immunol.* **202**, 360–367 (2019).
3. K. A. Richards *et al.*, Evidence that blunted CD4 T-cell responses underlie deficient protective antibody responses to influenza vaccines in repeatedly vaccinated human subjects. *J. Infect. Dis.* **222**, 273–277 (2020).
4. A. T. DiPiazza *et al.*, A novel vaccine strategy to overcome poor immunogenicity of avian influenza vaccines through mobilization of memory CD4 T cells established by seasonal influenza. *J. Immunol.* **203**, 1502–1508 (2019).
5. F. Krammer, The human antibody response to influenza A virus infection and vaccination. *Nat. Rev. Immunol.* **19**, 383–397 (2019).
6. D. M. Jelley-Gibbs *et al.*, Unexpected prolonged presentation of influenza antigens promotes CD4 T cell memory generation. *J. Exp. Med.* **202**, 697–706 (2005).
7. B. L. Bautista *et al.*, Short-lived antigen recognition but not viral infection at a defined checkpoint programs effector CD4 T cells to become protective memory. *J. Immunol.* **197**, 3936–3949 (2016).
8. J. Xia, Y. Kuang, J. Liang, M. Jones, S. L. Swain, Influenza vaccine-induced CD4 effectors require antigen recognition at an effector checkpoint to generate CD4 lung memory and antibody production. *J. Immunol.* **205**, 2077–2090 (2020).
9. P. Eldi, G. Chaudhri, S. L. Nutt, T. P. Newsome, G. Karupiah, Viral replicative capacity, antigen availability via hematogenous spread, and high  $T_{FH}$ : $T_{FR}$  ratios drive induction of potent neutralizing antibody responses. *J. Virol.* **93**, e01795-18 (2019).
10. S. R. Allie, T. D. Randall, Pulmonary immunity to viruses. *Clin. Sci. (Lond.)* **131**, 1737–1762 (2017).
11. T. M. Strutt *et al.*, Multipronged CD4(+) T-cell effector and memory responses cooperate to provide potent immunity against respiratory virus. *Immunity* **Rev. **255**, 149–164 (2013).**

**Virus Stocks, Infections, and Immunizations.** IAVs A/Puerto Rico/8/34 (PR8), originally from St. Jude Children's Hospital, and A/PR8-OVA<sub>II</sub>, kindly provided by Dr. Peter Doherty, were grown and maintained at the Trudeau Institute. Other viruses - LAIV, attenuated ca.A/Alaska/72/CR9 (ca.Alaska) (H3N2) and IBV, B/Ann Arbor/1/66 were originally supplied by S. Epstein (National Institutes of Health, Bethesda, MD) and grown in the Trudeau Institute. Mice were immunized i.n. with 2,500 median tissue culture infectious dose (TCID<sub>50</sub>) ca.A-laska as in our previous study (7) on d 0 and both i.n. and i.v. on d 6 to ensure that Ag is supplied to the spleen. Formalin-IIV (A/PR/8/34 [H1N1]) was purchased from Charles River Laboratories (material no. 10100782) and used at a dose of 10 µg i.v. as in our previous studies (8). Mice were anesthetized with isoflurane (Piramal Healthcare) or with ketamine/xylazine (at a dose of 25/2.5 mg/kg by i.p. injection) and were infected i.n. with influenza virus corresponding to a 0.2 to 0.3 medial lethal dose (LD<sub>50</sub>) dose of IAV in 50 µL of phosphate buffered saline (PBS).

In vivo-generated 6-d CD4 T cell effectors were routinely obtained as described previously (7). An in-depth description is provided in the *SI Appendix*.

**In Vivo APC Delivery.** To deliver Ag/APC (bone marrow derived DC [BMDC] or activated B cells), APCs were pulsed with 10 µM OVA<sub>323–339</sub> (OVA<sub>II</sub>) peptide (New England Peptide) or no peptide as a negative control (unpulsed APCs) for 1 h at 37°C with shaking. APCs were washed and administered either i.v. in 200 µL PBS, i.n. in 50 µL PBS, or i.s. in 10 µL PBS. A total of 0.25 × 10<sup>6</sup> to 1 × 10<sup>6</sup> BMDC or 1 × 10<sup>6</sup> B cells were transferred i.v., 0.5 × 10<sup>6</sup> to 2 × 10<sup>6</sup> BMDC or 1 × 10<sup>6</sup> to 2 × 10<sup>6</sup> B cells were transferred i.n., and 0.5 × 10<sup>6</sup> to 1 × 10<sup>6</sup> B cells were transferred i.s. Details about the i.s. APC transfer are provided in the *SI Appendix*.

Flow cytometry and enzyme-linked immunosorbent assays (ELISAs) were performed as described previously (51). An in-depth description is provided in the *SI Appendix*.

**Study Approval.** Experimental animal procedures were done in accordance with University of Massachusetts Medical School (UMMS) Animal Care and Use Committee guidelines that meet Institutional Animal Care and Use Committee (IACUC) guidelines.

**Data Availability.** All study data are included in the article and/or *SI Appendix*.

**ACKNOWLEDGMENTS.** We thank Dr. Richard Dutton, Dr. Kai McKinstry, and Dr. Tara Strutt for insightful discussions. We thank Dr. Jillian Richmond and Dr. Uthaman Gowthaman for manuscript feedback. We also thank Dr. Esteban Rozen, Yi Kuang, Jialing Liang, and Mike Perkins for assistance with experiments and animal husbandry. This work was supported by Grants U19 AI109858, P01 AI046530, R01 AI118820, and R21 AI128606 to S.L.S.; T32 AI007349 to A.M.V., O.K.-U., and M.C.J.; and R25 GM113686 and T32 AI132152 to O.K.-U.

12. C. G. Vinuesa, M. A. Linterman, D. Yu, I. C. MacLennan, Follicular helper T cells. *Annu. Rev. Immunol.* **34**, 335–368 (2016).
13. E. K. Deenick *et al.*, Follicular helper T cell differentiation requires continuous antigen presentation that is independent of unique B cell signaling. *Immunity* **33**, 241–253 (2010).
14. D. Baumjohann *et al.*, Persistent antigen and germinal center B cells sustain T follicular helper cell responses and phenotype. *Immunity* **38**, 596–605 (2013).
15. H. H. Tam *et al.*, Sustained antigen availability during germinal center initiation enhances antibody responses to vaccination. *Proc. Natl. Acad. Sci. U.S.A.* **113**, E6639–E6648 (2016).
16. J. Merkenschlager *et al.*, Dynamic regulation of  $T_{FH}$  selection during the germinal centre reaction. *Nature* **591**, 458–463 (2021).
17. K. K. McKinstry *et al.*, Effector CD4 T-cell transition to memory requires late cognate interactions that induce autocrine IL-2. *Nat. Commun.* **5**, 5377 (2014).
18. J. K. Krishnaswamy, S. Alsén, U. Yrlid, S. C. Eisenbarth, A. Williams, Determination of T follicular helper cell fate by dendritic cells. *Front. Immunol.* **9**, 2169 (2018).
19. D. Malhotra, A. L. Fletcher, S. J. Turley, Stromal and hematopoietic cells in secondary lymphoid organs: Partners in immunity. *Immunity* **Rev. **251**, 160–176 (2013).**
20. S. Crotty, T follicular helper cell differentiation, function, and roles in disease. *Immunity* **41**, 529–542 (2014).
21. M. Künzli *et al.*, Long-lived T follicular helper cells retain plasticity and help sustain humoral immunity. *Sci. Immunol.* **5**, eaay5552 (2020).
22. N. Fazilleau, L. J. McHeyzer-Williams, H. Rosen, M. G. McHeyzer-Williams, The function of follicular helper T cells is regulated by the strength of T cell antigen receptor binding. *Nat. Immunol.* **10**, 375–384 (2009).
23. J. Y. Lee *et al.*, The transcription factor KLF2 restrains CD4<sup>+</sup> T follicular helper cell differentiation. *Immunity* **42**, 252–264 (2015).
24. N. Swarnalekha *et al.*, T resident helper cells promote humoral responses in the lung. *Sci. Immunol.* **6**, eabb6808 (2021).

25. B. Pulendran, M. S. Maddur, Innate immune sensing and response to influenza. *Curr. Top. Microbiol. Immunol.* **386**, 23–71 (2015).
26. M. Terajima, J. A. Babon, M. D. Co, F. A. Ennis, Cross-reactive human B cell and T cell epitopes between influenza A and B viruses. *Virology* **10**, 244 (2013).
27. P. Devarajan *et al.*, New insights into the generation of CD4 memory may shape future vaccine strategies for influenza. *Front. Immunol.* **7**, 136 (2016).
28. K. Miyauchi *et al.*, Protective neutralizing influenza antibody response in the absence of T follicular helper cells. *Nat. Immunol.* **17**, 1447–1458 (2016).
29. I. Broadley, A. Pera, G. Morrow, K. A. Davies, F. Kern, Expansions of cytotoxic CD4<sup>+</sup>CD28<sup>-</sup> T cells drive excess cardiovascular mortality in rheumatoid arthritis and other chronic inflammatory conditions and are triggered by CMV infection. *Front. Immunol.* **8**, 195 (2017).
30. N. Gensous *et al.*, T follicular helper cells in autoimmune disorders. *Front. Immunol.* **9**, 1637 (2018).
31. D. Botta *et al.*, Dynamic regulation of T follicular regulatory cell responses by interleukin 2 during influenza infection. *Nat. Immunol.* **18**, 1249–1260 (2017).
32. M. Kitano *et al.*, Bcl6 protein expression shapes pre-germinal center B cell dynamics and follicular helper T cell heterogeneity. *Immunity* **34**, 961–972 (2011).
33. J. Shi *et al.*, PD-1 controls follicular T helper cell positioning and function. *Immunity* **49**, 264–274.e4 (2018).
34. J. P. Weber *et al.*, ICOS maintains the T follicular helper cell phenotype by down-regulating Krüppel-like factor 2. *J. Exp. Med.* **212**, 217–233 (2015).
35. G. Barbet *et al.*, Sensing microbial viability through bacterial RNA augments T follicular helper cell and antibody responses. *Immunity* **48**, 584–598.e5 (2018).
36. A. Ballesteros-Tato, T. D. Randall, Priming of T follicular helper cells by dendritic cells. *Immunol. Cell Biol.* **92**, 22–27 (2014).
37. E. K. Deenick, C. S. Ma, R. Brink, S. G. Tangye, Regulation of T follicular helper cell formation and function by antigen presenting cells. *Curr. Opin. Immunol.* **23**, 111–118 (2011).
38. T. N. Khan, J. L. Mooster, A. M. Kilgore, J. F. Osborn, J. C. Nolz, Local antigen in non-lymphoid tissue promotes resident memory CD8<sup>+</sup> T cell formation during viral infection. *J. Exp. Med.* **213**, 951–966 (2016).
39. S. R. Allie *et al.*, The establishment of resident memory B cells in the lung requires local antigen encounter. *Nat. Immunol.* **20**, 97–108 (2019).
40. S. R. McMaster *et al.*, Pulmonary antigen encounter regulates the establishment of tissue-resident CD8 memory T cells in the lung airways and parenchyma. *Mucosal Immunol.* **11**, 1071–1078 (2018).
41. S. Takamura *et al.*, Specific niches for lung-resident memory CD8<sup>+</sup> T cells at the site of tissue regeneration enable CD69-independent maintenance. *J. Exp. Med.* **213**, 3057–3073 (2016).
42. N. Pardi *et al.*, Nucleoside-modified mRNA vaccines induce potent T follicular helper and germinal center B cell responses. *J. Exp. Med.* **215**, 1571–1588 (2018).
43. S. Ndeupen *et al.*, The mRNA-LNP platform's lipid nanoparticle component used in preclinical vaccine studies is highly inflammatory. *iScience* (2021). 10.1016/j.isci.2021.103479.
44. T. J. Moyer, A. C. Zmolek, D. J. Irvine, Beyond antigens and adjuvants: Formulating future vaccines. *J. Clin. Invest.* **126**, 799–808 (2016).
45. K. M. Cirelli, S. Crotty, Germinal center enhancement by extended antigen availability. *Curr. Opin. Immunol.* **47**, 64–69 (2017).
46. K. M. Cirelli *et al.*, Slow delivery immunization enhances HIV neutralizing antibody and germinal center responses via modulation of immunodominance. *Cell* **177**, 1153–1171.e28 (2019).
47. A. V. Boopathy *et al.*, Enhancing humoral immunity via sustained-release implantable microneedle patch vaccination. *Proc. Natl. Acad. Sci. U.S.A.* **116**, 16473–16478 (2019).
48. G. A. Roth *et al.*, Injectable hydrogels for sustained codelivery of subunit vaccines enhance humoral immunity. *ACS Cent. Sci.* **6**, 1800–1812 (2020).
49. M. J. Barnden, J. Allison, W. R. Heath, F. R. Carbone, Defective TCR expression in transgenic mice constructed using cDNA-based alpha- and beta-chain genes under the control of heterologous regulatory elements. *Immunol. Cell Biol.* **76**, 34–40 (1998).
50. B. Scott *et al.*, A role for non-MHC genetic polymorphism in susceptibility to spontaneous autoimmunity. *Immunity* **1**, 73–83 (1994).
51. C. Kamperschroer, J. P. Dibble, D. L. Meents, P. L. Schwartzberg, S. L. Swain, SAP is required for Th cell function and for immunity to influenza. *J. Immunol.* **177**, 5317–5327 (2006).